First-principles studies of structures and stabilities of Pb/Si(111)

Tzu-Liang Chan, C. Z. Wang, M. Hupalo, M. C. Tringides, Zhong-Yi Lu,* and K. M. Ho
Ames Laboratory-U.S. Department of Energy, Iowa State University, Ames, Iowa 50011, USA
and Department of Physics and Astronomy, Iowa State University, Ames, Iowa 50011, USA
(Received 25 March 2003; revised manuscript received 7 May 2003; published 10 July 2003)

Various structures of Pb/Si(111) from 1/6 ML to 4/3 ML are investigated using first-principles calculations. Our calculations for the 1/6-ML mosaic phase and 1/3-ML β-phase yield good agreement with the experimental results. The higher coverage range $1/3 < \theta < 4/3$ ML has been controversial experimentally, especially close to 4/3 ML with several different phases being observed ($\sqrt{3}\times\sqrt{7}$, hexagonal incommensurate, striped incommensurate, etc.). We compare the unit cell energies of different structures to deduce the energetically favorable ones. Structures consisting of very flat Pb overlayers have lower energy than missing-top-layer structures or structures with stacking faults. This is in very good agreement with experiments which measure high Pb mobility on the α phase.

DOI: 10.1103/PhysRevB.68.045410 PACS number(s): 68.35.Bs, 73.20.Hb, 71.15.Mb

I. INTRODUCTION

The ordering of the two-dimensional epitaxial overlayer on a substrate is an interesting problem in physics.[1–4] One of the prototype systems for studying this type of problem is Pb/Si(111). It is known that Pb is not reactive with Si, and that they are mutually insoluble.[5–7] Pb/Si(111) can form a well-defined interface which is ideal for studying two-dimensional behavior. Both Pb and Si are group IV elements but their lattice constants are incommensurate. It is of great interest to understand what the resultant overlayer structure will be for different coverages of Pb on Si(111).

Experimentally, it turns out that the phase diagram of Pb/Si(111) is complicated, depending on coverage, temperature, and annealing history,[7–9] and Fig. 1 shows the different phases proposed by experiments between 1/6- and 4/3-ML coverages. For a Pb coverage of 1/6 ML, experiments observed the so-called mosaic phase (or γ phase), in which Pb and Si adsorb on T4 sites in equal proportion.[10,11] As the coverage increases, the adsorbed Si atoms at the T4 sites are gradually replaced by Pb atoms until all the Si atoms are replaced.[12] This is the β phase, which has a coverage of 1/3 ML. The β phase has a $\sqrt{3}\times\sqrt{3}$ symmetry with Pb atoms adsorbed on the T4 sites. Upon cooling below room temperature at 1/3-ML coverage, a 3×3 phase is observed.[9,13] The exact nature of the transition from the $\sqrt{3}\times\sqrt{3}\beta$ phase to the (3×3) phase is not clear, but it may be related to the charge density wave instability.[14–17] At 2/3 ML, Le Lay *et al.* observed a stable phase, and the proposed structure has a $\sqrt{3}\times\sqrt{3}$ symmetry with two Pb atoms adsorbed at T4 sites.[7] Since then, no other groups reported this particular phase at this coverage. At 1 ML, domains composed of $\sqrt{3}\times\sqrt{3}$ unit cells are observed.[18,19] STM experiments observed alternating domains of trimers with quasi-(1×1) region in between.[18] Two types of trimer domain are observed. The trimers are composed of three Pb atoms at T1 sites displaced either towards H3 or T4 sites. At high temperature, a commensurate-incommensurate transition from trimer domains to the (1×1) phase is observed. For coverage between 1 and 4/3 ML, a hexagonal incommensurate (HIC) phase, and a striped incommensurate (SIC) phase are observed.[8,9] They are also known as α phases. The exact structure of the α phase is not well understood. Upon cooling of the α phase, a low temperature phase with $\sqrt{3}\times\sqrt{7}$ symmetry is observed.[9,12,13,20] Except for the 1/6-ML mosaic phase and the 1/3-ML β phase, there are controversies as to the exact coverage and the corresponding structures of the other phases.

The purpose of this paper is to explore the various proposed structural models and other plausible models for Pb coverage between 1/6 and 4/3 ML using first-principles calculations in order to determine the energetically stable Pb coverage and the corresponding energetically favorable geometries. This paper is divided into five sections. Section II describes the theoretical tools and settings that our calculations are based on. Section III describes the structures that we have calculated together with simulated scanning tunneling microscopy (STM) images for certain structures. In Sec. IV, the energetics of the structures mentioned in Sec. III will be discussed, and our results will be compared with experiments. Section V is the conclusion.

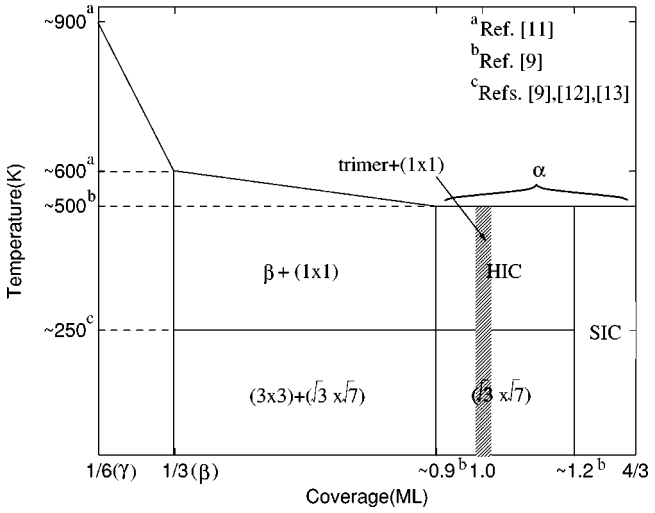

FIG. 1. Proposed phases of Pb/Si(111) by experiments for coverage between 1/6 and 4/3 ML.

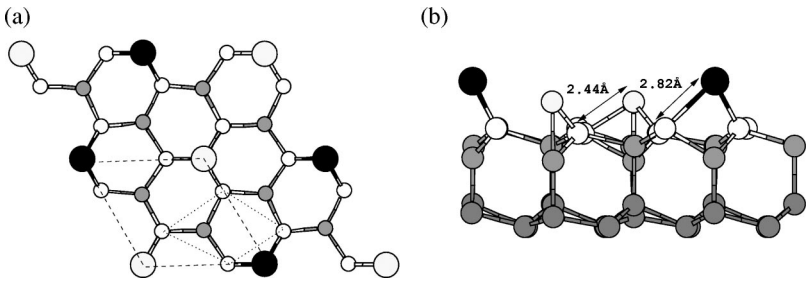

FIG. 2. (a) The top view and (b) side view of the 1/6-ML mosaic phase in a $2\sqrt{3}\times 2\sqrt{3}$ unit cell. Pb(Si) adatoms are black (light gray). Si atoms in the first (second and below) layer of the Si substrate are white (gray). Only the first two layers of the Si substrate are shown for the top view, with the Pb and Si adatoms represented by larger spheres. For the side view, top four layers of the Si substrate are shown. The 1×1 unit cell is indicated by a dotted line, and a dashed line for $\sqrt{3}\times\sqrt{3}$ unit cell. The top view and the side view are not in the same scale.

II. CALCULATION METHOD

Our first-principles calculations are based on density functional theory under local density approximations.[21] Pseudopotential and plane wave bases are being used. The Ceperley-Alder functional[22] parametrized by Perdew and Zunger[23] is used for the exchange-correlation energy functional. The kinetic energy cutoff is set to be 12 Ry. The Si(111) surface is modeled by a periodically repeating slab which consists of six layers of Si passivated by H at the bottom and a vacuum space of at least 12 Å. The bottom double layer of Si atoms is kept fixed to simulate the bulk environment, while all other atoms are allowed to relax until the forces are less than 0.025 eV/Å. A set of 48 special k points are chosen to sample the irreducible Brillouin zone of the 1×1 unit cell. For unit cells other than 1×1, equivalent k points have been used.

III. OPTIMIZED STRUCTURES

A. Structure of the mosaic phase at 1/6 ML

The 1/6-ML mosaic phase is modeled by a $2\sqrt{3}\times 2\sqrt{3}$ unit cell. The adsorbed atoms are located at T4 sites in which half of them are Pb and the other half are Si, as shown in Fig. 2 Our calculations show that this is a stable structure. Pb adatoms are higher than Si adatoms, resulting in a corrugation of 0.87 Å. The Pb-Si bond length is 2.82 Å, and the bond length between the Si adatom and Si substrate atom is 2.44 Å as shown in the figure. It should be noted that the Si adatoms are very close to the substrate, such that the Si atoms in the substrate directly below the adatoms are being pushed downwards relative to the other Si atoms in the same layer.

Simulated STM images[24] of this structure are shown in Fig. 3 The STM tip is assumed to position at a height of 2 Å above the highest atom in the structure. This assumption will be used for the other simulated STM images. Although Pb adatoms are higher than Si adatoms geometrically by 0.87 Å, the apparent height between them depends on the applied bias voltage. For negative bias voltages, there are only bright spots corresponding to Pb atoms. This is true for various bias voltages that we have tested between -0.5 and -2 V. Filled state images for -1 and -2 V are shown in Figs. 3(a) and 3(b), respectively. The situation is different for positive bias voltages. For an empty state image with a bias of 0.5 V [Fig. 3(c)], both Pb and Si atoms can be seen, although the spots corresponding to Si atoms are weaker. For voltages above 0.5 V [Fig. 3(d)], Pb adatoms are much brighter than Si. The dependence of the apparent height difference between Si and Pb on the sample bias was studied in Ref. 10, experimentally. For negative bias voltages, Ref. 10 has the same observation as our calculations. For positive bias voltages, the experiment observed the same apparent height for Pb and Si adatoms at 1.0 V. Pb adatoms look brighter than the Si adatoms for larger bias voltages. Although the precise bias voltages where Pb looks brighter than Si from the experiment is different from our calculation results, both the experiment and our calculations agree that there are changes on the apparent height between Pb and Si adatoms for positive bias voltages, but not for the negative case.

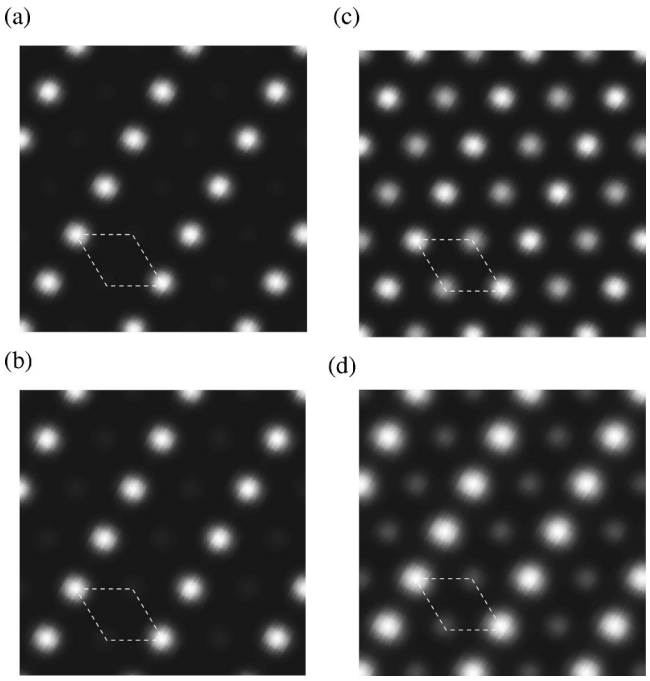

FIG. 3. Simulated STM images of the 1/6-ML mosaic phase with bias voltages of (a) -1.0 V, (b) -2.0 V, (c) 0.5 V, and (d) 1.0 V. The dashed lines indicate the same $\sqrt{3}\times\sqrt{3}$ unit cells as in Fig. 2(a).

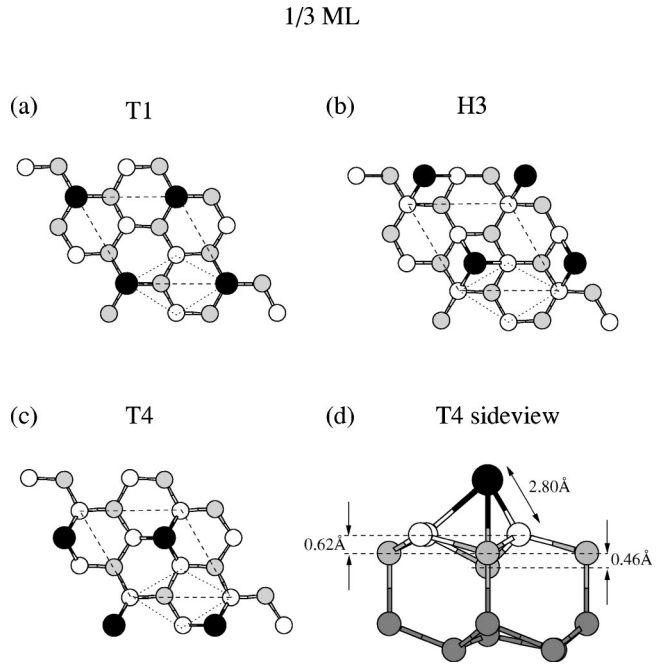

FIG. 4. (a) T1 model, (b) H3 model, (c) T4 model, and (d) side view of the T4 model for the 1/3-ML β phase. The top view and side view are not on the same scale. The scheme for coloring the atoms and outlining the unit cells is the same as Fig. 2.

B. Structures of the $\sqrt{3}\times\sqrt{3}$ phase at 1/3 ML

Three geometries based on the $\sqrt{3}\times\sqrt{3}$ unit cell are tested for a Pb coverage of 1/3 ML. They correspond to a Pb atom placed at the T1, H3, or T4 site, respectively, as shown in Fig. 4 Our calculations show that these three structures are all energetically stable, but the T4 structure is the most energetically favorable among the three. As one can see from Fig. 4(d), in the T4 structure the dangling bonds of the top Si layer of the substrate are all saturated by Pb adatoms. The Pb-Si bond length is 2.80 Å. The second layer of the Si substrate is 0.62 Å below the first layer, which is the same as a relaxed Si(111) substrate, but it is not flat. Those Si atoms which are directly below the T4 Pb adatoms are being pushed downwards by 0.46 Å relative to the other Si atoms in the second layer, and their distances to the Pb adatoms directly above is 2.93 Å. Simulated STM images of this structure are shown in Fig. 5. For both the empty state and occupied state images, there are bright spots corresponding to the T4 Pb atoms.

Since it is experimentally observed that there is a transition from the β phase to a 3×3 phase upon lowering the temperature, we studied the stability of the T4 structure by using a 3×3 unit cell, as shown in the inset of Fig. 6. The stability of the T4 model is tested with respect to a surface phonon distortion with 3×3 symmetry. We pick one Pb adatom, which is labeled A in the inset, fix its height, and all the other atoms are free to relax. This is repeated with different height of the chosen Pb adatom, and the result is shown in the plot of Fig. 6. If this surface phonon mode is soft, there will be a spontaneous distortion of the originally flat Pb overlayer. Our calculations show that the minimum in energy corresponds to a flat Pb layer. Simulated STM images for the

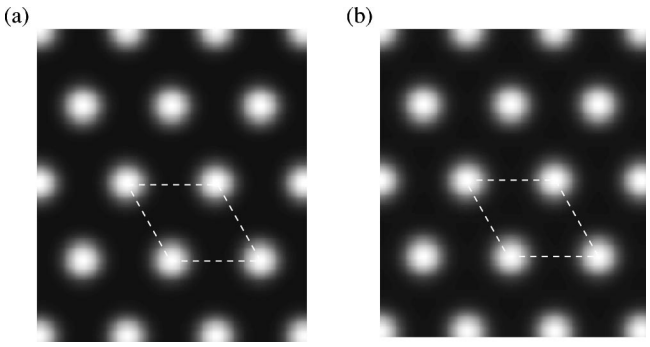

FIG. 5. Simulated STM images of the 1/3-ML β phase with bias voltages of (a) 1.0 V and (b) -1.0 V. The dashed lines indicate the same $\sqrt{3}\times\sqrt{3}$ unit cells as in Fig. 4(c).

T4 model with a 3×3 unit cell are also calculated. We found that all the bright spots have the same brightness, which look exactly the same as in Fig. 5. Even though a 3×3 unit cell is being used in the calculation, all results simply reduced to $\sqrt{3}\times\sqrt{3}$ symmetry both structurally and electronically.

C. Structures models at 2/3 ML

For a Pb coverage of 2/3 ML, our structural models consist of two Pb adatoms in a $\sqrt{3}\times\sqrt{3}$ unit cell. Each Pb adatom can be put on T1, T4, or H3 sites. Different ways of putting the two Pb adatoms on the three sites give six initial geometries. Upon relaxation, we found that when the two Pb atoms are placed at different sites, they will go off-site and dimerize with the other Pb atom. In particular, when Pb adatoms are located at T1 and T4 sites, the T4 Pb adatom will go to the bridge site. The Pb dimer has a bond length of 3.19 Å. When Pb adatoms are located at T1 and H3 sites, the H3 Pb adatom will also go to the bridge site to give the exact same structure as the previous case. When the Pb adatoms are put

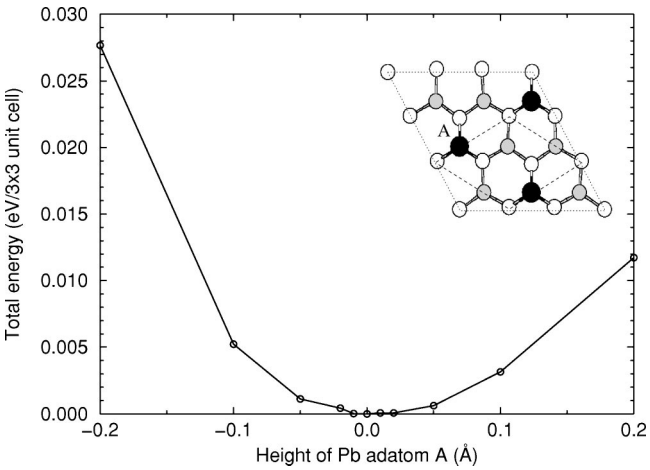

FIG. 6. A plot of the total energy of 1/3-ML 3×3 distorted T4 model vs the height of the labeled Pb adatom A. The total energy is with respect to that of the undistorted ground state structure. The inset shows the T4 model of the 1/3-ML β phase in a 3×3 unit cell, which is used for the calculations. The dotted line and the dashed line indicate the 3×3 and $\sqrt{3}\times\sqrt{3}$ unit cells, respectively. The scheme for coloring the atoms is the same as in Fig. 2.

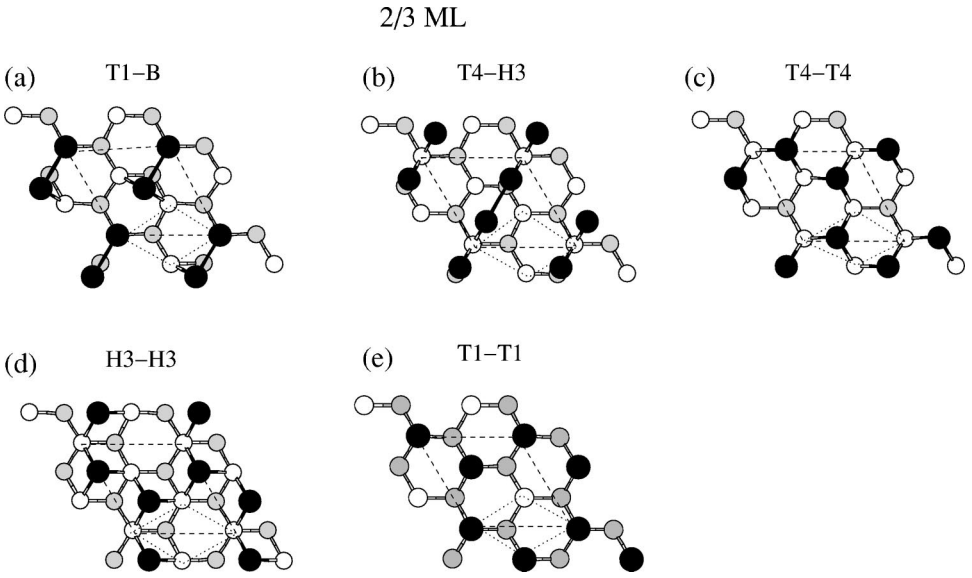

FIG. 7. (a) T1-B model, (b) T4-H3 model, (c) T4-T4 model, (d) H3-H3 model, and (e) T1-T1 model for 2/3-ML Pb coverage. The scheme for coloring the atoms and outlining the unit cells is the same as in Fig. 2.

at T4 and H3 sites, they will form a dimer with a length of 3.22 Å. Since two of the initial structures give the same final result, five stable structures are obtained as illustrated in Fig. 7. They are named according to where the Pb adatoms are located.

D. Structure models at 1 ML

The simplest models for 1 ML are structures based on 1×1 unit cells. Three structures are tested, in which a Pb adatom is placed at the T1, T4, or H3 site respectively. The T1 site is the most energetically stable structure among the three.[25] In this T1 model, the dangling bonds of the Si atoms in the first layer of the substrate are all saturated by Pb adatoms, with the Pb-Si bond length equal to 2.66 Å. The vertical distance between the first and second Si layers is 0.81 Å, which is bigger than 0.78 Å for an unrelaxed Si(111) substrate.

We also tested the trimer models based on the $\sqrt{3}\times\sqrt{3}$ unit cell. There are two proposed structures in Ref. 18 as shown in Figs. 8(a) and 8(b). Both contain Pb atoms adsorbed at T1 location but displaced a little bit off-site. If the Pb atoms displace towards the H3 site, we call the resultant structure the T^+ model. If it is towards the T4 site, it is called the T^- model. We found that it is energetically stable for the Pb atoms to be displaced either towards the T4 or H3 site. The bond length between Pb atoms in a trimer is 3.68 Å for the T^+ model and 3.74 Å for the T^- model, compared to 3.84 Å if the Pb atoms are located exactly at the T1 sites. The geometries of the T1 model and the trimer models are very similar. For both trimer models, the Pb-Si bond length is 2.68 Å, which is slightly bigger than the T1 model, and the distance between the first and second Si layers is 0.81 Å. An interesting difference between the T^- model and the other two models is that the second layer of the Si substrate of the T^- model is not completely flat. For the T^- model, the second layer Si atoms directly below the center of the Pb trimers is 0.02 Å lower than the rest of the Si atoms in the second layer.

Simulated STM images for the trimer models are shown in Fig. 9 For filled state images, clear distinct bright spots from Pb atoms can be observed for both T^+ and T^- models, while for empty state images, the bright spots are displaced away from the H3(T4) site and the intensity is low at the H3 (T4) position for the T^+ (T^-) model, although the Pb adatoms are displaced towards the H3 (T4) site structurally. At the same bias voltage of 1.0 V, the T^+ structure is about

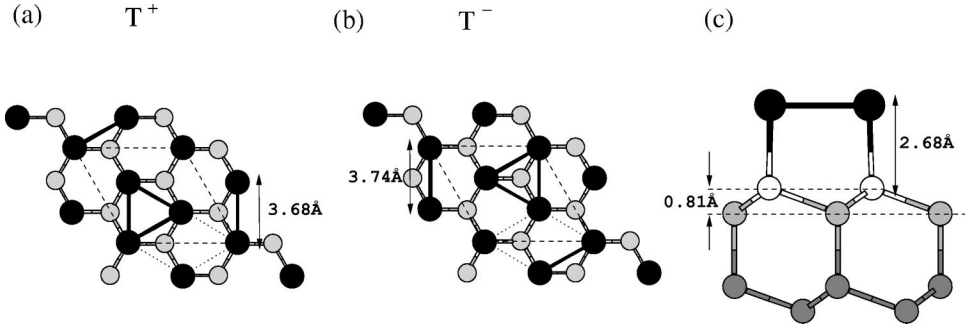

FIG. 8. The top view of (a) 1-ML T^+ and (b) T^- models. Their side view diagrams look exactly the same, and are illustrated in (c). Please refer to the text for the subtle difference between them. The top view and side view are not on the same scale. The scheme for coloring the atoms and outlining the unit cells is the same as Fig. 2.

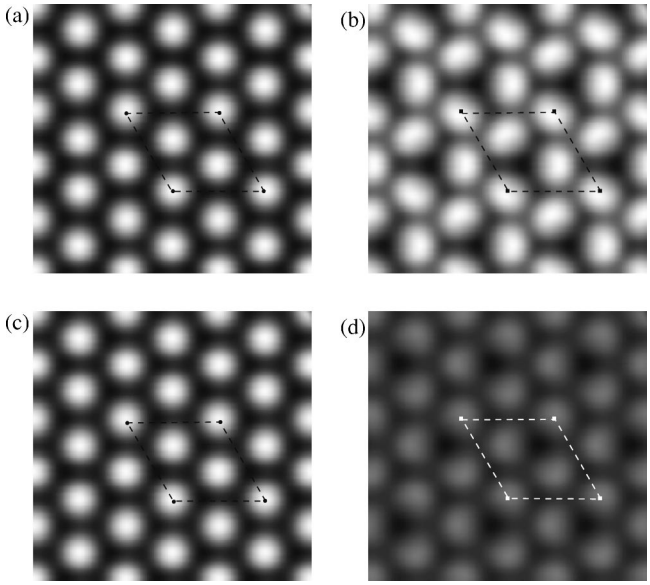

FIG. 9. Simulated STM images of the T^+ model with bias voltages of (a) -1.0 V and (b) 1.0 V. Simulated STM images for the T^- model is shown in (c) and (d) with bias voltages of -1.0 and 1.0 V respectively. The dashed lines indicate the same $\sqrt{3}\times\sqrt{3}$ unit cells as in Figs. 8(a) and 8(b). (b) and (d) are plotted under the same gray scale. The bright spots in (b) are around twice as bright as those in (d).

twice as bright as the T^- structure. If T^+ and T^- domains coexist in the same structure, they can be differentiated by their apparent height in STM empty state images.

Based on the results of Ag/Si(111) (Ref. 26) and Au/Si(111),[27] missing-top-layer (MTL) models for Pb/Si(111) may be possible. MTL models are structures with the first layer of the Si substrate removed such that each Si atom of the top layer has three dangling bonds. Four different MTL models are tested. The honeycomb-chained-trimer (HCT) model observed in Ag/Si(111) is shown in Fig. 10(a). The structure consists of chained Pb trimers with the centers of the trimers forming a honeycomb network. A related model is called the inequivalent-triangle (IET) model.[28] The difference between HCT and IET models is that for the IET model, the Pb and Si trimers are twisted such that the mirror plane symmetry along the $[11\bar{2}]$ direction is lost, while the three fold symmetry is preserved. We found that the IET

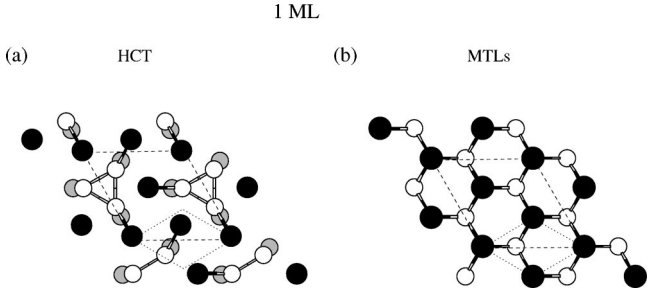

FIG. 10. (a) HCT model and (b) MTL model for the 1-ML α phase. The scheme for coloring the atoms and outlining the unit cells is the same as Fig. 2.

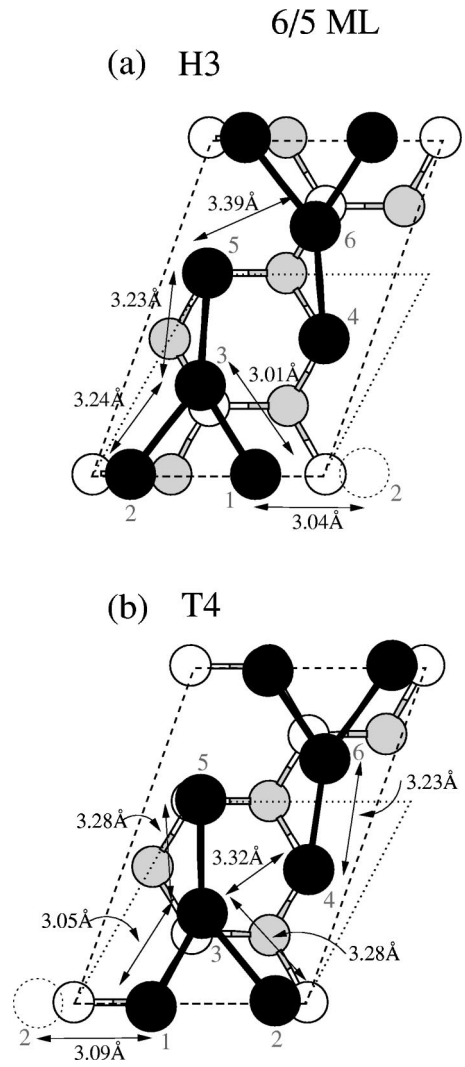

FIG. 11. (a) H3 model, and (b) T4 model based on $\sqrt{3}\times\sqrt{7}$ unit cell for the 6/5-ML Pb coverage. The dotted and dashed lines indicate the $\sqrt{3}\times\sqrt{3}$ and $\sqrt{3}\times\sqrt{7}$ unit cells, respectively. The labeling of the Pb adatoms for the H3 model is the same as that of Ref. 20. The Pb adatoms of the T4 model are labeled in the same way except that Pb adatom 1 denotes the T4 Pb adatom instead of the H3 Pb adatom. The dotted circles denotes Pb adatom 2 in the adjacent unit cell. The scheme for coloring the atoms is the same as Fig. 2.

model is not energetically stable and it relaxed to the model HCT. Another related structure is the conjugate-HCT (CHCT) model.[27] Instead of Pb atoms forming chained trimers, the CHCT model has the top layer of Si forming chained trimers instead. Our calculations found that the model CHCT is not energetically stable and reduced to the model HCT upon relaxation. The fourth MTL model that we considered is the substitution model (MTLs). We start with a Si(111) substrate with a top double layer. Then the first Si layer is replaced by Pb atoms such that the bonds of the second Si layer are all saturated. We found that the model MTLs is energetically stable and it is shown in Fig. 10(b).

E. Structure models at 6/5 ML

At low temperature and with a Pb coverage of 6/5 ML, a $\sqrt{3}\times\sqrt{7}$ phase have been observed. In our present calcula-

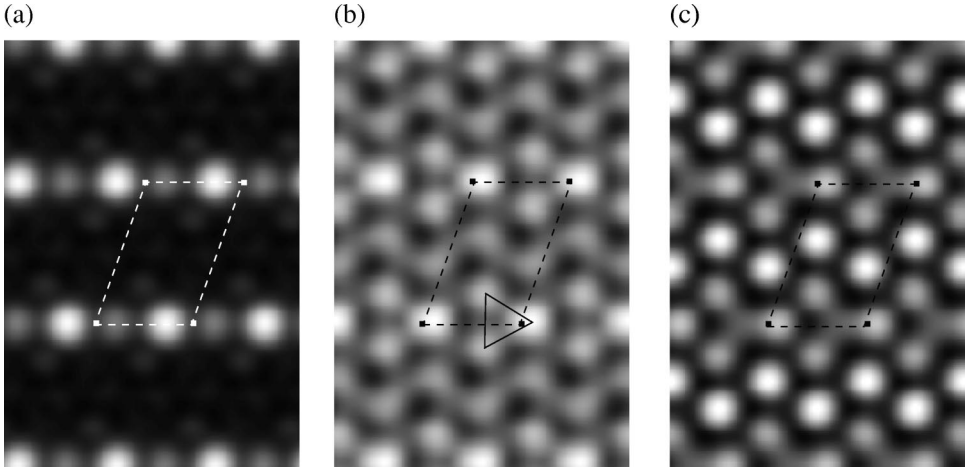

FIG. 12. Simulated STM images of the 6/5-ML H3 model with bias voltages of (a) 1.5 V, (b) −0.35 V, and (c) −1.0 V. The dashed lines indicate the same $\sqrt{3}\times\sqrt{7}$ unit cells as in Fig. 11. The triangle in (b) denotes a trimerlike feature that can be observed in the filled states image.

tions, we adopted the structure from the x-ray diffraction experiment[20] as shown in Fig. 11(a). There are six Pb atoms in a unit cell, one of them is at H3 site, the others are at T1 site or off-centered T1 site. We called this structure the H3 model. As we will show later in this paper when we compare the energetics of different structures, the energy difference between placing a Pb adatom at the H3 or T4 site is very small when the Pb coverage is above 1 ML; therefore we tested a competitive model in which the H3 Pb adatom is placed at the T4 site instead. The resultant structure is called the T4 model and is shown in Fig. 11(b). Both structures are energetically stable. A detailed description of the structure of H3 model can be found in Ref. 20 and theoretical studies on this structure have been done as well.[29] We repeat this calculation together with our newly proposed T4 model. From our calculations, the bond lengths between the H3 Pb adatom with the other Pb adatoms are 3.01 and 3.04 Å, which is close to the Pb-Pb covalent bond length of 2.94 Å. The other Pb-Pb bond lengths not involving the H3 Pb adatom are greater than 3.2 Å, which is closer to the metallic Pb bond length of 3.50 Å. The corrugation of the Pb overlayer is 0.14 Å. Our result is consistent with the previous theoretical study[29] and experimental observations in Ref. 20, which also observed that there may be more than one equilibrium height for the H3 Pb adatom. We did calculations to search for other possible heights for the H3 Pb adatom, but we cannot find another equilibrium position. For the T4 model, we can make similar observations that the bond lengths between the T4 Pb adatom and the other Pb adatoms are close to the Pb-Pb covalent bond length, while the other Pb-Pb bond lengths are more metallic. The corrugation of the Pb overlayer in the T4 model is 0.13 Å.

Simulated STM images for the H3 model are shown in Fig. 12. For empty state image [Fig. 12(a)], a bright spot corresponding to the H3 Pb adatom and a weaker spot corresponding to an off-site T1 Pb atom can be seen. For filled state images [Figs. 12(b) and 12(c)], five spots which seem to come from T1 position can be found in a unit cell. The relative brightness of these spots depend on the bias voltage. For the −0.35 V filled state image in Fig. 12(b), a trimerlike feature is observed, which is highlighted in the figure. We also calculated the simulated STM images for the T4 model, as shown in Fig. 13. As in the H3 model, a bright spot corresponding to the T4 Pb adatom can be observed in the empty state image. For the filled state image, spots corresponding to the other T1 Pb adatoms can be seen and their relative brightness also depend on the bias voltage, as shown in Figs. 13(b) and 13(c). We again noticed a trimerlike feature when the bias voltage is -0.35 V, but the orientation is different from that of the H3 model. Therefore, both H3 and T4 models should produce very similar features in STM images, and they can only be differentiated by the registry of

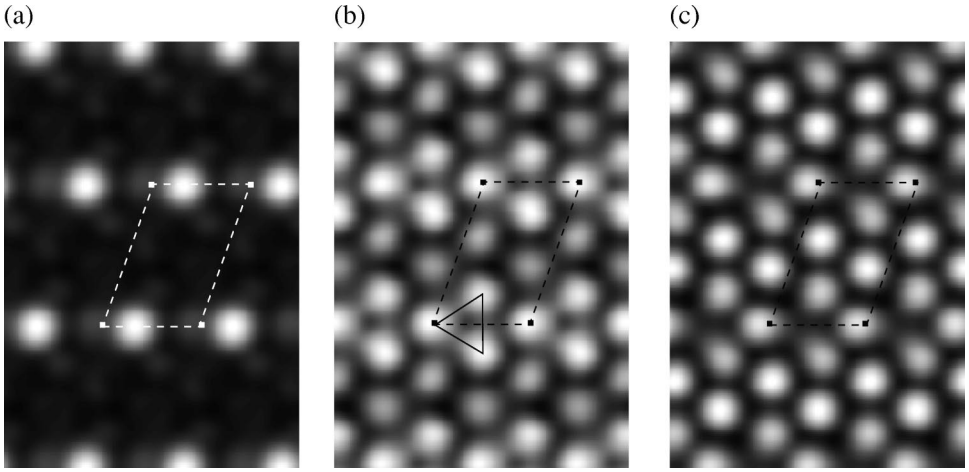

FIG. 13. Simulated STM images of the 6/5-ML T4 model with bias voltages of (a) 1.5 V, (b) -0.35 V, and (c) −1.0 V. The dashed lines indicate the same $\sqrt{3}\times\sqrt{7}$ unit cells as in Fig. 11. The triangle in (b) denotes a trimerlike feature that can be observed in the filled state image. Note that it is pointing in the opposite direction when compared to Fig. 12(b).

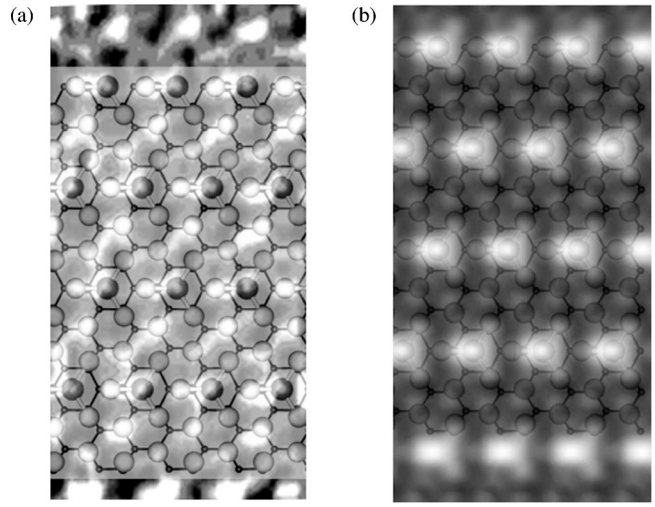

FIG. 14. Si(111) lattice and Pb adatoms overlaid on top of (a) a high-resolution STM image of the $\sqrt{3}\times\sqrt{7}$ phase with a bias voltage of 1.3 V, and (b) a simulated STM image of the H3 model at the same bias voltage. The small spheres represents the Si(111) lattice and the big spheres are the Pb adatoms. Bonds are drawn in between the H3 Pb adatoms and their adajacent T1 Pb adatoms, where the bond lengths are approximately 3 Å.

the bright spots with respect to the underlying Si(111) substrate. In Fig. 14, the Si(111) lattice(small spheres) and the Pb adatoms(big spheres) are overlaid on top of both the experimental and theoretical data. Figure 14(a) presents a high-resolution STM image of the $\sqrt{3}\times\sqrt{7}$ phase at a bias voltage of 1.3 V. Bright spots can be observed between H3 Pb adatoms and the adjacent T1 Pb adatoms; this feature is reproduced accurately by our calculation, as shown in Fig. 14(b). If the T4 model is the correct structure, the bright spots mentioned above would have to shift along the $(11\bar{2})$ direction by approximately half of the $\sqrt{3}$ lattice constant. This illustrates unambiguously that the H3 model fits the experimental STM results better than the T4 model. It can be noted that there are other bright spots corresponding to T1 Pb adatoms in the experimental STM image, which are absent in the theoretical calculation. However, these extra spots are also absent in a recent STM experiment of the $\sqrt{3}\times\sqrt{7}$ phase.[29] The reason for the difference between the results of the two STM experiments is not clear.

F. Structures of $\sqrt{3}\times\sqrt{3}$ H3 and T4 models at 4/3 ML

For 4/3 ML coverage, we consider structures based on $\sqrt{3}\times\sqrt{3}$ unit cells with four Pb atoms in each unit cell. The first structure is called the H3 model, in which one Pb atom is located at the H3 site and the other three at the off-centered T1 location forming a trimer. It is energetically stable and is shown in Fig. 15. The Pb overlayers essentially form a flat surface, which is about 2.6 Å above the Si substrate. The vertical distance between the first and second layer Si substrates is 0.82 Å. The H3 Pb adatom has a bond length of 3.03 Å with its nearest Pb adatoms. The trimers formed by the off-centered T1 Pb adatoms have a length of 3.38 Å. By replacing the H3 Pb atom by a Pb atom on the T4 site, we obtain another model called the T4 model. It is also energetically stable and is shown in Fig. 16. The Pb overlayer is again very flat, with a corrugation of 0.23 Å, and about 2.6 Å above the Si substrate. The vertical distance between the first and second layers of Si substrate is 0.86 Å, with the second layer Si atoms which are directly below the T4 Pb adatoms 0.1 Å higher than the rest of Si atoms in the same layer. The T4 Pb adatom has a bond length of 3.09 Å with its nearest Pb adatoms. The trimers has a length of 3.45 Å for this case.

Simulated STM images are shown in Figs. 17(a)–17(d). Empty state images show bright spots corresponding to H3 (T4) Pb atom for the H3 (T4) model. From Fig. 17, we can see that the H3 model gives brighter spots than the T4 model. If a H3 domain and a T4 domain coexist on the same structure, they can be differentiated by their apparent height in STM. For occupied states images, bright spots corresponding to the other three Pb atoms on the T1 sites can be seen for both models. But the occupied state image of the H3 model has a substantial intensity at the H3 positions, while very little intensity is seen at the T4 positions in the T4 model.

We also found another energetically stable structure which is neither H3 nor T4, but looks similar to them. It has a Pb atom at an off-site T4 location and another at off-site H3 location, as shown in Fig. 18. The Pb adatoms form chain-like structures along the $[11\bar{2}]$ direction. We call this structure the intermediate (Int) phase, as it looks like a transition state between the H3 and T4 models. The Pb overlayer has a corrugation of 0.15 Å and it is around 2.58 Å above the Si substrate. As shown in Fig. 18(a), the bond length is 3.20 Å between Pb-1 and Pb-2, 3.19 Å between Pb-2 and Pb-3, and 2.94 Å between Pb-3 and Pb-1. The vertical distance between the first two layers of the Si substrate is 0.81 Å. The Si atoms in the second layer of the substrate below Pb-1 are slightly higher than the rest of the Si atoms in the same layer by 0.1 Å.

Simulated STM images of the Int phase are shown in Figs. 17(e) and 17(f). One bright spot and one weaker spot

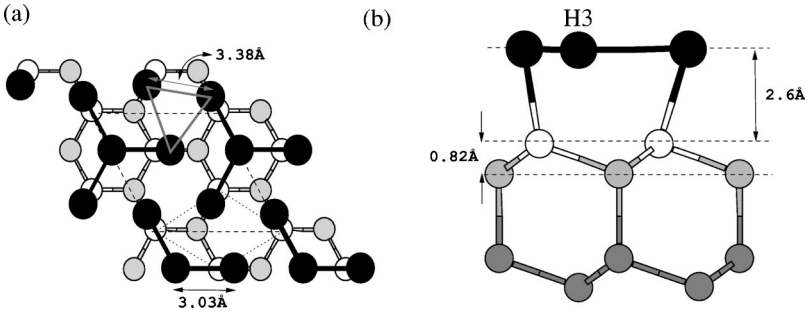

FIG. 15. (a) The top view and (b) side view of the 4/3-ML H3 model. The gray-bordered triangle in (a) illustrates the trimers formed by the off-centered T1 Pb adatoms as mentioned in the text. The side view illustrates the Pb adatom at H3 position(the labeled Pb adatom) and its nearest Pb adatoms. The top view and the side view are not in the same scale. The scheme for coloring the atoms and outlining the unit cells is the same as Fig. 2.

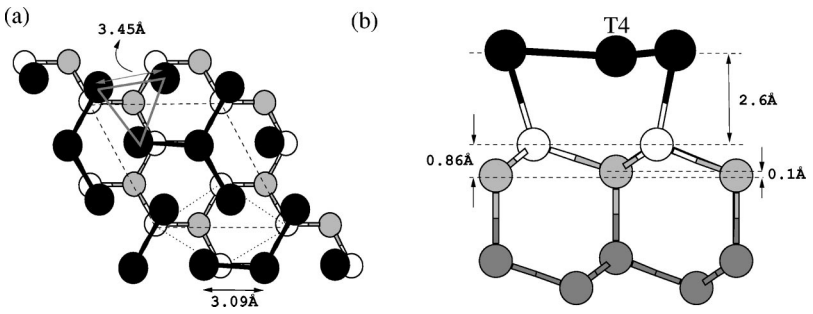

FIG. 16. (a) The top view and (b) side view of the 4/3-ML T4 model. The gray-bordered triangle in (a) illustrates the trimers formed by the off-centered T1 Pb adatoms as mentioned in the text. The side view illustrates the Pb adatom at T4 position(the labeled Pb adatom) and its nearest Pb adatoms. The top view and the side view are not in the same scale. The scheme for coloring the atoms and outlining the unit cells is the same as Fig. 2.

can be found in a unit cell in the empty state image. The brighter spots come from the off-site T4 Pb atom and the weaker spots come from the off-site H3 Pb atoms. The filled state image gives three spots in a unit cell: two bright spots and a weaker elongated spot. The weaker spots come from the off-site H3 Pb atom and extend to the T1 site towards the off-site T4 Pb atom, which does not give a bright spot in the filled state image. The two bright spots come from the other two Pb atoms located near the T1 sites in the unit cell.

As for 1 ML, we also consider the possibility of MTL models. A simple extension from the 1-ML MTL models to 4/3-ML structures is obtained by adding one extra Pb adatom to the $\sqrt{3}\times\sqrt{3}$ unit cell. In this way, we obtained energetically stable HCT-adatom models (HCTa1, HCTa2) and MTL-substitution-adatom models (MTLsa-H3, MTLsa-T4), as shown in Fig. 19. Since these four models are obtained by putting an additional Pb adatom on top of the existing 1ML MTL models, the Pb overlayer has a large corrugation. Structural models with small corrugations of the Pb overlayer are also constructed by simply removing the first Si layer in the Si(111) substrate of the 4/3-ML H3 and T4 models. The Pb overlayer from the H3 and T4 models are lowered to a reasonable height and laterally displaced as a whole with respect to the missing-top-layer substrate. Since it is not obvious what lateral displacement will give the lowest energy structure, we generated many $\sqrt{3}\times\sqrt{3}$ MTL models with flat Pb overlayers and the only difference between them is that the Pb overlayer is laterally displaced as a whole with respect to the MTL substrate. Among the flat MTL models that we have generated in the above manner, the most energetically favorable one after optimization is shown in Fig. 19(a), which we call the MTL1 model. Finally, we consider the H3 and T4 models with stacking fault (H3sf, T4sf) on the Si(111) substrate. The relative energetics of these structures will be considered in the following section.

IV. RELATIVE STABILITIES

We have calculated the formation energies of the structures discussed in Sec. III in order to compare their relative stabilities. The formation energy is defined as

$$E_s=(E-E_{sub}-N_{Pb}\times E_{Pb}-Nsi\times E_{si})/A, \qquad (1)$$

where E is the total energy of the structure, E_{sub} is the total energy of the Si(111) substrate, $N_{Pb}(N_{Si})$ is the number of Pb(Si) adatoms in a unit cell, $E_{Pb}(E_{Si})$ is the total energy of a bulk Pb (Si) atom in a fcc (diamond) structure, and A is the surface area of the Si(111) substrate. This formula measures the stability of a structure with respect to a clean Si(111) substrate and with Pb and Si adatoms in their respective bulk environment. If the formation energy is negative, it is energetically favorable to form that particular structure.

For structures based on MTL models, their formation energies are not obtained from Eq. (1). Since the Si(111) substrate with a missing top layer has three dangling bonds per surface atom, it has a much higher energy than a substrate with a top double layer. A direct application of Eq. (1) to

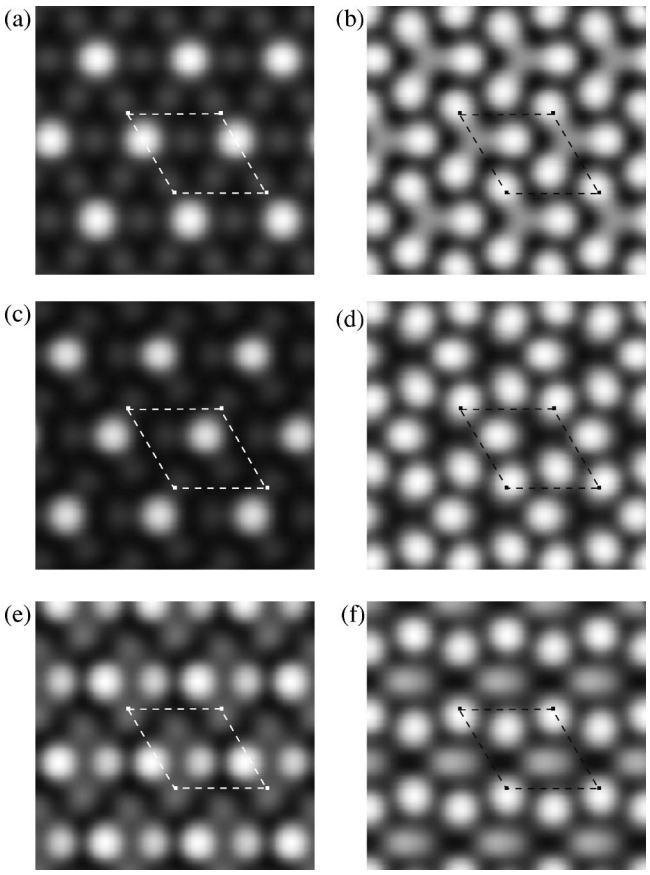

FIG. 17. Simulated STM images of the 4/3-ML H3 model with bias voltages of (a) 1.5 V and (b) −1.5 V. For the 4/3-ML T4 model, the simulated STM images are shown in (c) for 1.5 V and (d) for −1.5 V. While for the 4/3-ML Int model, it is (e) and (f) for 2.0 and −1.5 V, respectively. The dashed lines indicate the same $\sqrt{3}\times\sqrt{3}$ unit cells as in Fig. 15 for the H3 model, Fig. 16 for the T4 model, and Fig. 18 for the Int model. It should be noted that (a) and (c) are plotted under the same gray scale. We can see that the H3 spots are brighter than the T4 spots.

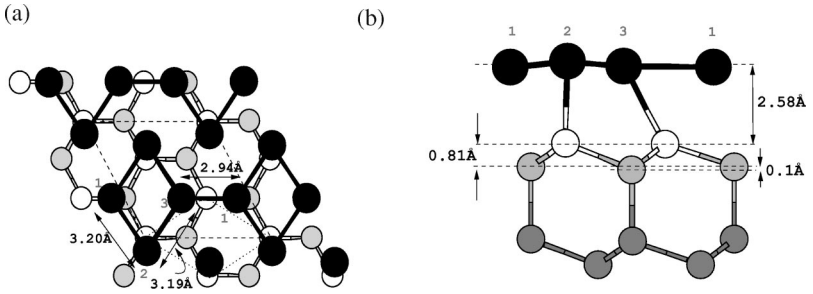

FIG. 18. (a) The top view and (b) side view of the 4/3-ML Int model. The top view and side view are not on the same scale. The scheme for coloring the atoms and outlining the unit cells is the same as in Fig. 2.

MTL models does not allow a fair comparison with other models. We use an indirect method to infer the formation energies of MTL models. For a given MTL model, a corresponding structure with inversion symmetry is generated, such that hydrogen passivation at the bottom of the substrate is not necessary. Then we pick another non-MTL structure at the same Pb coverage and generate a structure with inversion symmetry. These two structures with inversion symmetry should have the same number of Pb and Si atoms in a unit cell, such that the total energies can be directly compared. Since the formation energy of the other chosen structure is known from Eq. (1), the formation energy of the MTL model can be inferred from the total energy difference. For MTL models to be formed, the top layer of the Si(111) has to be removed when Pb is deposited. The physical interpretation of the formation energy for MTL models is that the removed top Si atoms are assumed to go to a bulk diamond Si environment.

The formation energies of all the structures mentioned in Sec. III are summarized in Table I and illustrated in Fig. 20. For 1/6 ML, the mosaic phase has a negative formation energy, therefore it is energetically favorable to form this structure. For 1/3 ML, the T4 model has the lowest formation energy, which is 0.14 eV lower than the H3 model. The T1 model is not energetically favorable. This agrees with the experimental observations that the β phase consists of Pb atoms adsorbed at T4 sites. For 2/3 ML, the coexistence between the β phase and the $\sqrt{3}\times\sqrt{7}$ phase is observed experimentally. From our calculations, the T1-B and T4-T4 models are the lowest energy structures and they are degenerate in energy. If a stable phase at 2/3 ML can be observed, T1-B model is a possible candidate apart from the T4-T4 model proposed by Le Lay *et al.*[7] For 1 ML, the T1 model and the trimer models (T^+,T^-) are the most favorable and they are degenerate in energy. Contrary to Ag/Si(111) and Au/Si(111), MTL models are not as favorable in this case. For 6/5 ML, the H3 model is slightly lower in energy than the T4 model by 0.01 eV per 1×1 unit cell. Experimentally, only the H3 model is observed. Despite the similarity between the adsorption energies at H3 and T4 sites of the $\sqrt{3}\times\sqrt{7}$ phase, only domains with H3 sites are observed both in x-ray and STM experiments. However, as we have shown in a recent publication for the HIC structure[30] which has $\theta=1.25$ ML (built with $\sqrt{3}\times\sqrt{3}$ unit cells in the domain interior and essentially the $\sqrt{3}\times\sqrt{7}$ phase in the domain walls), both H3 and T4 sites are observed. It is still not clear why the binding site of the $\sqrt{3}\times\sqrt{7}$ phase is only H3 while for the HIC phase, which easily evolves from the $\sqrt{3}\times\sqrt{7}$ phase with the addition of few monolayer percent of Pb, both sites are occupied.

For 4/3 ML, the T4, H3, and Int models are the lowest energy structures, and they are nearly degenerate in energy. There are a few interesting implications from our results for 4/3 ML. The first point is that although for a clean Si(111) (1×1) surface, the energy for a stacking fault is 0.04 eV, as shown in Table I, the Pb overlayer seems to stabilize the stacking fault. The energies of T4sf and H3sf models are

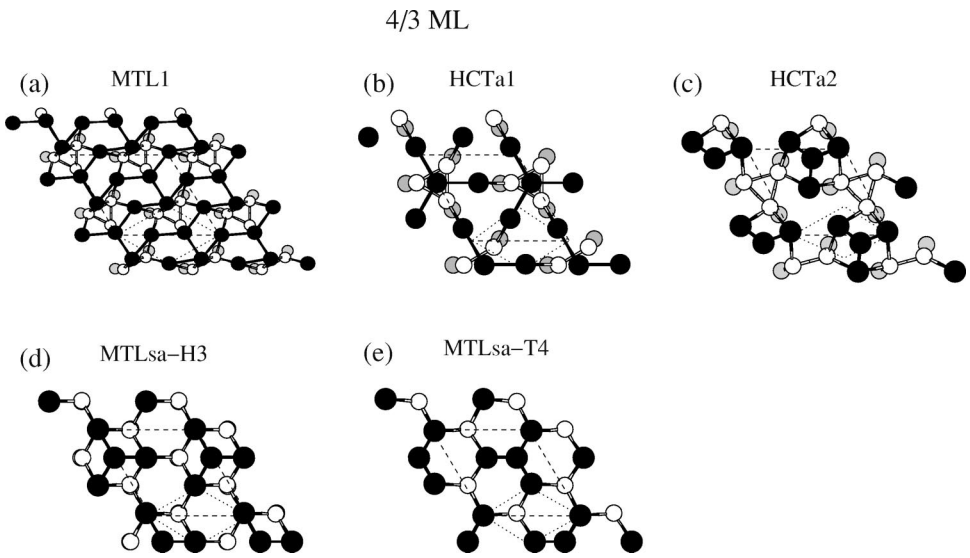

FIG. 19. (a) MTL1 model, (b) HCTa1 model, (c) HCTa2 model, (d) MTLsa-H3 model, and (e) MTLsa-T4 model for the 4/3 ML α phase. The scheme for coloring the atoms and outlining the unit cells is the same as in Fig. 2.

TABLE I. Formation energies of the energetically stable structures from 1/6 to 4/3 ML. The formation energy of the stacking fault is included as a reference.

Coverage	Unit cell	Name of structure	E_s (eV per 1×1 unit cell)
0	1×1	stacking fault	0.04
1/6	$2\sqrt{3}\times2\sqrt{3}$	mosaic	−0.43
1/3	$\sqrt{3}\times\sqrt{3}$	T4	−0.51
		H3	−0.37
		T1	0.16
2/3	$\sqrt{3}\times\sqrt{3}$	T1-B	−0.34
		T4-T4	−0.34
		H3-H3	−0.26
		T4-H3	−0.23
		T1-T1	−0.06
1	1×1	T1	−0.47
		H3	−0.21
		T4	−0.20
	$\sqrt{3}\times\sqrt{3}$	T^+	−0.47
		T^-	−0.47
		HCT	−0.39
		MTLs	−0.14
6/5	$\sqrt{3}\times\sqrt{7}$	H3	−0.70
		T4	−0.69
4/3	$\sqrt{3}\times\sqrt{3}$	T4	−0.76
		H3	−0.75
		Int	−0.76
		T4sf	−0.75
		H3sf	−0.74
		HCTa1	−0.23
		HCTa2	−0.17
		MTLsa-H3	0.01
		MTLsa-T4	−0.06
		MTL1	−0.40

only 0.01 eV higher than their unfaulted counterpart. It is generally believed that when Pb is deposited on Si(111) 7×7, stacking fault will be removed. Our calculations show that this might not be the case. The second point is the apparent height difference between the H3 and T4 models in the STM empty state image, and their degeneracy in energy can be used to explain the features observed in the HIC phase. The HIC phase is believed to be composed of alternating domains of H3 and T4 models. This will be further discussed elsewhere.[30] Finally, the Int model bears a close resemblance to the T4 and H3 models as described in Sec. III. In addition, its energy is nearly degenerate with the T4 and H3 models. The Int model may act as a bridge between T4 domains and H3 domains. In particular, the Int model may be related to the domain wall structure of the HIC phase.

The third point is that the MTL models are not as energetically favorable as the other models as in 1 ML. The

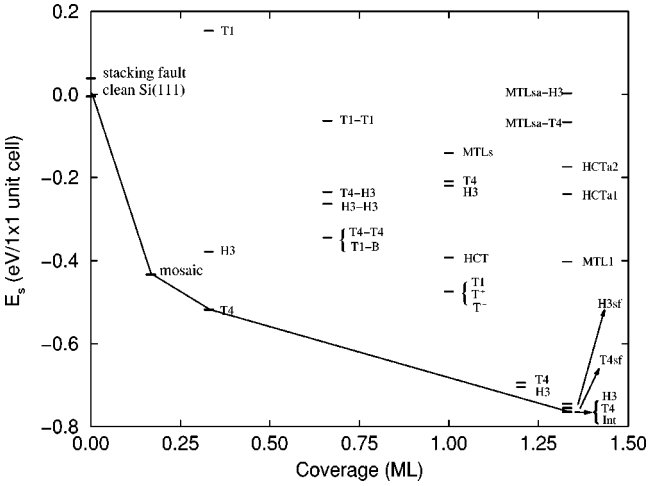

FIG. 20. A plot of the formation energies of various models against Pb coverage on Si(111). A linear interpolation is done between certain lowest energy structures with different coverages. An explanation for the interpolation can be found in the text.

lowest energy structure among the MTL models is the MTL1 model. One of the differences between MTL1 and other MTL models is that the Pb overlayer in MTL1 has a smaller corrugation, while the others are highly corrugated as mentioned in Sec. III. This feature is shared by the H3, T4, Int, and stacking faults models, in which the corrugation of the Pb overlayer is less than 0.25 Å. These structures may comprise the wetting layer on which three-dimensional Pb islands can grow. The flatness may provide low diffusion barrier which facilitates the growth of 3D islands.[31–33] Fig. 21 shows a STM image of the SIC phase which consists of $\sqrt{3}\times\sqrt{3}$ domains separated by meandering domain walls, which are essentially $\sqrt{3}\times\sqrt{7}$ unit cells.[33] The coverage is slightly above 4/3 ML. The smoothness of this image is consistent with the above calculated value. Growth of additional Pb on top of this phase at even lower temperatures, $100<T$

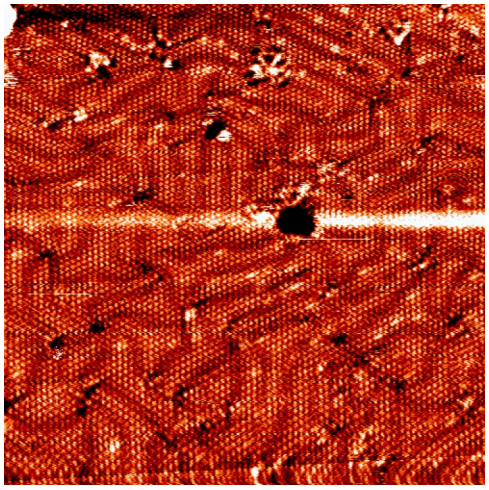

FIG. 21. Different domains of $\sqrt{3}\times\sqrt{3}$ separated by meandering domain walls which are essentially $\sqrt{3}\times\sqrt{7}$ unit cells. The corrugation of the phase is 0.05 nm, in good agreement with the calculation.

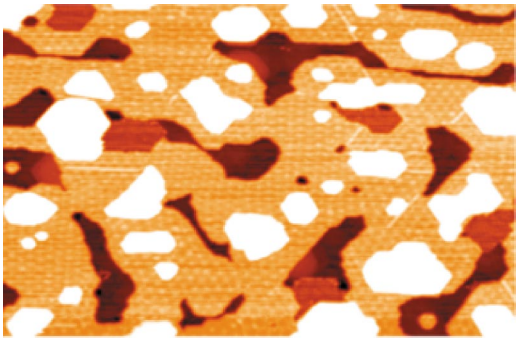

FIG. 22. 147×95-nm^2 STM image showing the formation of a long flat 2-step film with few 4-step islands on top at $T=160$ K and $\theta=4$ ML (including the amount of Pb in the $\sqrt{3}\times\sqrt{3}\alpha$ phase). This is an indication of the high Pb mobility on the α phase.

<240 K, results in the formation of well-ordered regular structures extending up to 100 nm in linear size. First, networks of planar triangular Pb clusters will form when small extra amount of Pb is deposited ($\Delta\theta<1$ ML). For larger amount of Pb deposited ($\Delta\theta>1$ ML) with increasing temperature, (111)-oriented Pb islands grow by bilayer height increments as a result of quantum-size effects. Figure 22 shows the result of the growth after depositing ~2.5 ML of Pb on top of the well-annealed α phase at 150 K. A 2-step film grows first, extending over the whole 147×95-nm^2 image, with the next four-step layer forming on top of it, thus providing experimental evidence for the low corrugation of the $\sqrt{3}\times\sqrt{3}\alpha$ phase and also the low diffusion barrier of this phase. The modulation observed on top of the islands is an electronic effect related to variations at the metal/semiconductor interface discussed elsewhere.[34]

Up till now, we compared structures with the same coverage. A comparison of structures with different coverage can be done as follows. From Fig. 20, the points corresponding to the lowest energy structures of 1/6, 1/3, and 4/3 ML are linearly interpolated. The interpolation between 1/3 and 4/3 ML, for example, represents domains with 1/3 ML coexisting with domains with 4/3 ML. If we assume the domain wall density is low, the energy associated with them can be neglected. This justifies the use of a linear interpolation between structures. The structures with 2/3, 1, and 6/5 ML are above the interpolated curves. This implies that they are susceptible to segregation into domains of 4/3 and 1/3 ML, and therefore, they are not stable coverage. The conclusion for 2/3 ML agrees with the fact that nearly all experimental groups did not observe a stable 2/3-ML phase. Although the 1-ML phase is observed experimentally, it is not a stable coverage according to our analysis. This discrepancy may be due to the fact that our energetics are based on local $\sqrt{3}\times\sqrt{3}$ or 1×1 geometries, assuming a negligible contribution from domain walls. This may not be applicable to the experimentally observed 1-ML phase. It is also possible that the observed 1-ML phase is metastable. Our results show that the 6/5-ML models are not stable, this is contradictory to the experimental fact that the $\sqrt{3}\times\sqrt{7}$ H3 model is observed upon cooling at a Pb coverage between 1/3 ML and around 1.2 ML. A reversible phase transition at $T\sim270$ K has been found with several techniques(X-ray and STM) with $\sqrt{3}\times\sqrt{7}$ being the stable phase at 6/5 ML and $T<270$ K. It is still not clear what the high temperature phase for $T>270$ K and the nature of the phase transition is, whether it is the HIC (Ref. 9) or the disordered 1×1 phase.[12] In addition, in the range of $1/3<\theta<6/5$ ML, experimentally there is coexistence between the 1/3-ML 3×3 phase and the $\sqrt{3}\times\sqrt{7}$ phase at low temperature. One possibility for the discrepancy between experimental and theoretical results is that there is a different structure for the $\sqrt{3}\times\sqrt{7}$ phase than the one we have used in the calculation, i.e., the one based on the H3 binding site and 6/5 ML is not the lowest energy structure. Although our calculations for this model yield good agreement with both x-ray and STM experiments,[29] it is possible that another lower energy structure exists which can produce similar diffraction and STM results. We adopted the proposed structure directly from Ref. 20 without an extensive search for other possible geometries at this coverage. Since the $\sqrt{3}\times\sqrt{7}$ phase is only about 20 meV above the interpolated curve, it is also possible that the local density approximation cannot resolve such a small energy difference. Yet another clue as to why in the calculation the $\sqrt{3}\times\sqrt{7}$ phase is above the interpolated energy between the 1/3-ML β phase and the 4/3-ML α phase can be obtained from the recent discovery of numerous ordered phases in the range $1.2<\theta<1.33$ ML, differing by minute amounts in coverage and built hierarchically according to the formation rules of the ''devil's staircase.''[35] Such phases are built by combining integral numbers n, m of the two generating phases of coverages θ_1 and θ_2, i.e., the $\sqrt{3}\times\sqrt{7}$ phase with $\theta_1=1.2$ ML and the $\sqrt{3}\times\sqrt{3}\alpha$ phase with $\theta_2=1.33$ ML. Any such phases will have coverage $\theta=1+[(n+m)/(5n+3m)]$ within the range $1.2<\theta<1.33$. Twelve such phases have been resolved by STM within $\Delta\theta\sim0.1$ ML, one of the best realizations of the ''devil's staircase'' so far. More details of how the phases are constructed can be found elsewhere,[35] but the important observation for our current discussion is that these phases result from long range elastic interactions because of the large mismatch between Pb and Si lattice constants ($\sim9\%$). The energy due to these elastic interactions falls off with distance $J(r)\sim1/r^2$, and it is not included in our calculated energy of the structures, which extends only up to one unit cell with the periodic boundary conditions being imposed. This missing part of the elastic energy is repulsive and favors larger unit cells with a larger average separation between the atoms. The contribution of the elastic energy will raise the energy of a structure by an amount which increases with the nominal coverage of the structure, since the average atom separation decreases with increasing nominal coverage, i.e., the energy of the 4/3-ML $\sqrt{3}\times\sqrt{3}$ structures will increase more than the energy of the 6/5-ML $\sqrt{3}\times\sqrt{7}$ structures. The repulsive elastic energy of the structure with coverage θ_2 being higher than that with θ_1 is a necessary condition for the numerous phases corresponding to the ''devil's staircase'' to form. The net result is to reduce the slope of the coexistence straight line between 1/3 and 4/3 ML. This will therefore raise the energy corresponding to the phase with the 1/3- and 4/3-ML structures coexisting higher

than the energy of the $\sqrt{3}\times\sqrt{7}$ H3 structure. In addition, as discussed before, the region $6/5<\theta<4/3$ ML is not simply phases of coexisting regions between the $\sqrt{3}\times\sqrt{7}$ and $\sqrt{3}\times\sqrt{3}\alpha$ phases, but an infinite number of phases with coverages equal to any rational number between θ_1 and θ_2. Because the system experiences long range interactions, the energy of the system is lowered if the separation between the unit cells of the two generating phases are arranged in well-defined patterns, i.e., the separation between the unit cells of one type is as uniform as possible for a given coverage. This will be discussed in detail elsewhere.[35,36]

V. CONCLUSION

By using first-principles calculations, various models of Pb/Si(111) from 1/6 to 4/3 ML are studied, including existing proposed models, MTL models, and models with stacking faults. Our theoretical results have good agreement for both 1/6 and 1/3 ML. We successfully predict that 1/6 and 1/3 ML are stable Pb coverages while 2/3 ML is not. Between 1 and 4/3 ML, our calculations indicate that energetically favorable structures consist of very flat Pb overlayer, missing-top-layer models are not likely, and models with stacking faults may be possible. Further studies with a more extensive search of possible structures at these coverage are required.

ACKNOWLEDGMENTS

Ames Laboratory is operated for the U.S. Department of Energy by Iowa State University under Contract No. W-7405-Eng-82. This work was supported by the Director for Energy Research, Office of Basic Energy Sciences including a grant of computer time at the National Energy Research Supercomputing Center (NERSC) in Berkeley and CCS at Oak Ridge National Laboratory.

*Present address: Department of Physics and Astronomy, Vanderbilt University, Nashville, Tennessee 37235, USA.

[1] F.C. Frank, and J.H. Van Der Merwe, Proc. R. Soc. London, Ser. A **198**, 205 (1949).
[2] P. Bak, Rep. Prog. Phys. **45**, 587 (1982).
[3] J. Villain, Surf. Sci. **97**, 219 (1980).
[4] J. Villain, in *Ordering in Strongly Fluctuating Condensed Matter Systems* edited by T. Riste (Plenum, New York, 1980), p. 221.
[5] G. Le Lay, J. Peretti, M. Hanbucken, and W.S. Yang, Surf. Sci. **204**, 57 (1988).
[6] R.W. Olesinki and G.J. Abbaschian, Bull. Alloy Phase Diagrams **5**, 271 (1984).
[7] G. Le Lay, M. Abraham, A. Kahn, K. Hricovini, and J.E. Bonnet, Phys. Scr. **T35**, 261 (1991).
[8] L. Seehofer, G. Falkenberg, D. Daboul, and R.L. Johnson, Phys. Rev. B **51**, 13 503 (1995).
[9] K. Horikoshi, X. Tong, T. Nagao, and S. Hasegawa, Phys. Rev. B **60**, 13 287 (1999).
[10] J.M. Gomez-Rodriguez, J.-Y. Veuillen, and R.C. Cinti, Surf. Sci. **377-379**, 45 (1997).
[11] E. Ganz, I.-S. Hwang, F. Xiong, K. Silva Theiss, and J. Golovchenko, Surf. Sci. **257**, 259 (1991).
[12] J. Slezak, P. Mutombo, and V. Chab, Phys. Rev. B **60**, 13 328 (1999).
[13] O. Custance, J.M. Gomez-Rodriguez, A.M. Baro, L. Jure, P. Mallet, and J.-Y. Veuillen, Surf. Sci. **482-485**, 1399 (2001).
[14] G. Ballabio, G. Profeta, S. de Gironcoli, S. Scandolo, G.E. Santoro, and E. Tosatti, Phys. Rev. Lett. **89**, 126803 (2002).
[15] L. Petaccia, L. Floreano, A. Goldoni, D. Cvetko, A. Morgante, L. Grill, A. Verdini, G. Comelli, G. Paolucci, and S. Modesti, Phys. Rev. B **64**, 193410 (2001).
[16] R. Perez, J. Ortega, and F. Flores, Phys. Rev. Lett. **86**, 4891 (2001).
[17] J.M. Carpinelli, H.H. Weitering, M. Bartkowiak, R. Stumpf, and E.W. Plummer, Phys. Rev. Lett. **79**, 2859 (1997).
[18] I.S. Hwang, R.E. Martinez, C. Liu, and J.A. Golovchenko, Phys. Rev. B **51**, 10 193 (1995).
[19] A. Petkova, J. Wollschlager, H.-L. Gunter, and M. Henzler, Surf. Sci. **471**, 11 (2001).
[20] C. Kumpf, O. Bunk, J.H. Zeysing, M.M. Nielsen, M. Nielsen, R.L. Johnson, and R. Feidenhans'l, Surf. Sci. **448**, L213 (2000).
[21] P. Hohenberg and W. Kohn, Phys. Rev. **136**, B864 (1964); W. Kohn and L.J. Sham, *ibid.* **140**, A1135 (1965).
[22] D.M. Ceperley and B.J. Alder, Phys. Rev. Lett. **45**, 566 (1980).
[23] J.P. Perdew and A. Zunger, Phys. Rev. B **23**, 5048 (1981).
[24] J. Tersoff, and D.R. Hamann, Phys. Rev. B **31**, 805 (1985).
[25] The relative energetics between different sites in 1×1 unit cells are calculated by other groups as well; see, for example, Ref. 29.
[26] Y.G. Ding, C.T. Chan, and K.M. Ho, Phys. Rev. Lett. **67**, 1454 (1991).
[27] Y.G. Ding, C.T. Chan, and K.M. Ho, Surf. Sci. Lett. **275**, L691 (1992).
[28] H. Aizawa, M. Tsukada, N. Sato, and S. Hasegawa, Surf. Sci. **429**, L509 (1999).
[29] S. Brochard, E. Artacho, O. Custance, I. Brihuega, A.M. Baro, J.M. Soler, and J.M. Gomez-Rodriguez, Phys. Rev. B **66**, 205403 (2002).
[30] M. Hupalo, T.L. Chan, C.Z. Wang, K.M. Ho, and M.C. Tringides, Phys. Rev. B **66**, 161410 (2002).
[31] M. Hupalo, V. Yeh, L. Berbil-Bautista, S. Kremmer, E. Abram, and M.C. Tringides, Phys. Rev. B **64**, 155307 (2001).
[32] M. Hupalo, S. Kremmer, V. Yeh, L. Berbil-Baustista, E. Abram, and M.C. Tringides, Surf. Sci. **493**, 526 (2001).
[33] M. Hupalo and M.C. Tringides, Phys. Rev. B **65**, 205406 (2002).
[34] M. Hulapo (unpublished).
[35] M. Hupalo, J. Schmalian, and M.C. Tringides, Phys. Rev. Lett. **90**, 216106 (2003).
[36] J. Schmalian, M. Hupalo, and M.C. Tringides (unpublished).